

NBS REPORT

6751

RECEIVED
LIBRARY
APR 17 1961

S. H. Simpson, Jr.

VHF AND UHF SIGNAL CHARACTERISTICS OBSERVED ON
A LONG KNIFE-EDGE DIFFRACTION PATH

by

PROPERTY OF
SOUTHWEST RESEARCH INSTITUTE LIBRARY
SAN ANTONIO, TEXAS

A. P. Barsis and R. S. Kirby



U. S. DEPARTMENT OF COMMERCE
NATIONAL BUREAU OF STANDARDS
BOULDER LABORATORIES
Boulder, Colorado

THE NATIONAL BUREAU OF STANDARDS

Functions and Activities

The functions of the National Bureau of Standards are set forth in the Act of Congress, March 3, 1901, as amended by Congress in Public Law 619, 1950. These include the development and maintenance of the national standards of measurement and the provision of means and methods for making measurements consistent with these standards; the determination of physical constants and properties of materials; the development of methods and instruments for testing materials, devices, and structures; advisory services to government agencies on scientific and technical problems; invention and development of devices to serve special needs of the Government; and the development of standard practices, codes, and specifications. The work includes basic and applied research, development, engineering, instrumentation, testing, evaluation, calibration services, and various consultation and information services. Research projects are also performed for other government agencies when the work relates to and supplements the basic program of the Bureau or when the Bureau's unique competence is required. The scope of activities is suggested by the listing of divisions and sections on the inside of the back cover.

Publications

The results of the Bureau's work take the form of either actual equipment and devices or published papers. These papers appear either in the Bureau's own series of publications or in the journals of professional and scientific societies. The Bureau itself publishes three periodicals available from the Government Printing Office: The Journal of Research, published in four separate sections, presents complete scientific and technical papers; the Technical News Bulletin presents summary and preliminary reports on work in progress; and Basic Radio Propagation Predictions provides data for determining the best frequencies to use for radio communications throughout the world. There are also five series of nonperiodical publications: Monographs, Applied Mathematics Series, Handbooks, Miscellaneous Publications, and Technical Notes.

Information on the Bureau's publications can be found in NBS Circular 460, Publications of the National Bureau of Standards (\$1.25) and its Supplement (\$1.50), available from the Superintendent of Documents, Government Printing Office, Washington 25, D.C.

APR 17 '61

S. H. Shapiro, Jr.

NATIONAL BUREAU OF STANDARDS REPORT

NBS PROJECT

8370-11-83171

March 1, 1961

NBS REPORT

6751

VHF AND UHF SIGNAL CHARACTERISTICS OBSERVED ON
A LONG KNIFE-EDGE DIFFRACTION PATH

by

A. P. Barsis and R. S. Kirby



U. S. DEPARTMENT OF COMMERCE
NATIONAL BUREAU OF STANDARDS
BOULDER LABORATORIES
Boulder, Colorado

IMPORTANT NOTICE

NATIONAL BUREAU OF STANDARDS
Approved for public release by the
Director of the National Institute of
Standards and Technology (NIST) on
October 9, 2015.
Documents intended for use within
is subjected to additional eval-
uation, or open-literature listing
mission is obtained in writing
25, D. C. Such permission is
been specifically prepared if

progress accounting docu-
s is formally published it
tion, reprinting, reproduc-
not authorized unless per-
of Standards, Washington
for which the Report has
es for its own use.

TABLE OF CONTENTS

| | <u>Page No.</u> |
|---|-----------------|
| Summary | 1 |
| 1. Introduction | 1 |
| 2. Characteristics of the Received Signal and Variation of Hourly Median Values | 2 |
| 2.1 Signal Characteristics | 2 |
| 2.2 Variations of Hourly Medians | 2 |
| 2.3 Comparative Studies of Median Distributions | 3 |
| 2.4 Frequency Dependence of the Distributions of Hourly Medians | 6 |
| 3. Height Gain Studies | 6 |
| 4. Vertical Space Diversity and Fading Characteristics | 8 |
| 5. Conclusions | 9 |
| 6. Acknowledgements | 10 |
| 7. Table of References | 10 |

VHF AND UHF SIGNAL CHARACTERISTICS OBSERVED ON A LONG KNIFE-EDGE DIFFRACTION PATH

by

A. P. Barsis and R. S. Kirby
National Bureau of Standards
Boulder, Colorado

Summary

During 1959 and 1960 long-term transmission loss measurements were performed over a 223 kilometer path in Eastern Colorado using frequencies of 100 and 751 Mc. This path intersects Pikes Peak which forms a knife-edge type obstacle visible from both terminals. The transmission loss measurements have been analyzed in terms of diurnal and seasonal variations in hourly medians and in instantaneous levels. As expected, results show that the long-term fading range is substantially less than expected for tropospheric scatter paths of comparable length. Transmission loss levels were in general agreement with predicted knife-edge diffraction propagation when allowance is made for rounding of the knife edge. A technique for estimating long-term fading ranges is presented and the results are in good agreement with observations. Short-term variations in some cases resemble the space-wave fadeouts commonly observed on within-the-horizon paths, although other phenomena may contribute to the fading. Since the foreground terrain was rough, there was no evidence of direct and ground-reflected lobe structure.

In most cases comparatively high correlation exists between signals received simultaneously on two antennas with 8, 3 and 14 meters vertical separation. These separations were chosen as being representative for practical space diversity systems designed for eliminating the effects of fading arising from direct and ground reflected phase interference phenomena. The comparatively high correlation observed suggests that space diversity will be relatively less successful in mountain obstacle paths with rough terrain near the terminals than on tropospheric scatter paths or on line-of-sight paths over smooth terrain.

The enhancement of field strength associated with propagation over mountain ridges may cause concern in applications where mountains are being counted on to shield unwanted radio waves. Some radio astronomy installations have been located in mountain valleys for this reason, and it is

possible that obstacle-gain effects may aggravate rather than alleviate interference.

1. Introduction

It is generally known that mountain ridges can act as diffracting knife-edges in point-to-point communication circuits on VHF and UHF frequencies. The mathematical approach was developed by Schelleng, Burrows, and Ferrel, using the Fresnel-Kirchhoff diffraction theory.¹ Substantial reductions in transmission loss as compared to scatter circuits of similar length, and relatively fading-free signals were reported by several workers, both in this country and abroad.²⁻⁷ More recently, additional work in Japan,⁸ and so far unpublished data from Alaskan knife-edge diffraction paths⁹ have shown that some paths exhibit considerable fading at carrier frequencies in the 900 Mc range. Much of the time the fading encountered resembles the "space-wave fadeout" phenomena observed commonly on within-the-horizon paths at comparable frequencies and first analyzed by Bean.¹⁰ It consists of relatively deep and slow fades, and the occurrence of these fades may show marked diurnal trends and correlation with meteorological phenomena as well as with simultaneous ducting on paths just beyond the horizon.

To obtain a better understanding of the long-term signal and fading characteristics, the National Bureau of Standards established a test path in Colorado to study knife-edge type diffraction phenomena. This path extends in a roughly north-south direction along the Front Range of the Colorado Rockies, and uses Pikes Peak as the diffracting knife-edge. An outline map of the path with the locations of the terminals at Beulah and Table Mesa, Colorado, is shown on Fig. 1. Pertinent path and equipment data are given in Table 1, below. The path profile is shown on Fig. 2, based on an equivalent earth radius of 9000 km. This is 1.41 times the actual earth's radius and corresponds to a surface refractivity of 316 N-units.

Table 1

Path and Equipment Data
Pikes Peak Obstacle Gain Path

| | |
|--|--|
| Path Distance..... | 223 km |
| Angular Distance..... | 64.4 milliradians |
| Terminal Elevations Above Mean Sea Level | |
| Transmitter..... | (Beulah) 1905 m |
| Receiver..... | (Table Mesa) 1666 m |
| Height of Obstruction Above Mean Sea Level | |
| (Pikes Peak)..... | 4292 m |
| Height of Obstruction Above Mean | |
| Receiver Height.... | 2507 m |
| Antenna Heights Above Ground | |
| Transmitter..... | 7.3 m for 751 Mc, 12.4 m for 100 Mc |
| Receiver..... | 8.2, 16.5 and 22.3 m for 751 Mc, 13.7 m for 100 Mc |
| Polarization..... | Horizontal |
| Antennas | |
| | 751 Mc 100 Mc |
| Transmitting | 4.3 m Dish Yagi |
| Receiving | 3 m Dish Yagi |
| Modulation | Continuous Wave |

Operation on 751 Mc commenced in December, 1959, and terminated in September, 1960. Data were recorded continuously during five-day periods at the rate of one each month with more frequent operation in June and August. Operation on 100 Mc started in August, 1960, on the same basis. During two five-day periods in August, 1960, an additional site was operated on top of Pikes Peak, using horizontal half-wave dipole receiving antennas on both frequencies. These antennas were mounted about 6 m above ground. The length of this auxiliary line-of-sight path was 77 km.

The receiver outputs were recorded on strip charts and multi-channel magnetic tape. Transmitter power output values were also recorded on strip charts, so that a continuous record of the transmitter power is available for both frequencies. The receivers were calibrated by signal generators checked against laboratory standards.

2. Characteristics of the Received Signal and Variation of Hourly Median Values

2.1 Signal Characteristics

Fig. 3 shows sample recordings of both frequencies at the two sites taken on the morning of August 10, 1960. The 751 Mc record at the Table

Mesa receiving site shows more rapid small signal variations superimposed on a much slower fading pattern, which includes a fade in excess of 15 db lasting several minutes. There appears to be substantial correlation between the signal recorded simultaneously on the two antennas on 751 Mc. The slow fading pattern is absent on the Table Mesa 100 Mc record; only the more rapid variations are present, and they are superimposed on a virtually constant signal. It is believed that these rapid signal variations of small amplitude are due to a component of scattered field superimposed on the more slowly varying diffracted field. For the line-of-sight path with the terminal on the top of Pikes Peak this scattered component is not noticeable, as expected. However, the slower variations are still present on 751 Mc, and they do not appear correlated with the slow fading observed at the Table Mesa site.

The slow signal variations which are similar to the "space-wave fadeouts" commonly observed on line-of-sight paths will be discussed in more detail later on.

2.2 Variations of Hourly Medians

A typical sample of diurnal variations of hourly medians is shown on Fig. 4 for the period August 8-12, 1960, at the Table Mesa receiving site. Each open circle denotes an hourly median of basic transmission loss for the hour given by the abscissa. The distribution of the points and the median curve shows no pronounced diurnal trend. This is in contrast to (smooth earth) diffraction or scatter paths of similar length where usually a substantial diurnal trend of hourly median values is observed.

Similarly, the absence of a pronounced seasonal trend is shown by Fig. 5. Here, the median of all hourly medians recorded during each five-day period is plotted vs time. The maximum variation is about 5 db. The overall medians obtained for the two antennas appear well correlated, and there seems to be no significant difference between the results obtained at the two heights used for the corner reflector antenna. During the three recording periods in June when the corner reflector antenna was at the 22.3 m elevation, the overall medians follow the trend given by the rest of the data, when the 16.5 m height was used.

The 100 Mc data at Table Mesa and the Pikes Peak data were not included in this study, because they are only available for August and September--not enough to study seasonal trends.

It should be recognized that the time periods on Fig. 5 are consecutive as far as recorded data are concerned. Weeks with no recordings have been omitted.

Diurnal and seasonal variations may also be studied by obtaining distributions of hourly medians for eight time blocks as defined by Norton, et al.¹¹ For this purpose, the hours of the day are divided into four blocks for summer as well as winter months, as follows:

Table 2
Time Blocks

| No. | Months | Hours |
|-----|------------------|-----------|
| 1 | November - April | 0600-1300 |
| 2 | November - April | 1300-1800 |
| 3 | November - April | 1800-2400 |
| 4 | May - October | 0600-1300 |
| 5 | May - October | 1300-1800 |
| 6 | May - October | 1800-2400 |
| 7 | May - October | 0000-0600 |
| 8 | November - April | 0000-0600 |

Cumulative distributions of the hourly basic transmission loss medians are calculated for each individual time block, or for combinations of time blocks, and plotted on log-normal graph paper. Thus it is possible to obtain an estimate of the range of observed hourly medians which is the long-term fading range. This will be compared with theoretical estimates, or with similar data obtained from other paths.

The cumulative distributions of all measured hourly median transmission loss values are

shown on Fig. 6 separately for all time blocks, and for both 751 Mc antennas, with the corner reflector at the 16.5 m elevation. All curves are bunched and nearly parallel, indicating very little diurnal or seasonal variation. Table 3, below, shows a comparison of the overall median values and the long-term fading range. Here the overall median is the median of all hourly medians within a time block, and the long-term fading range is defined as the difference between hourly median values exceeded 1% and 99% of all hours.

Even though the cumulative distributions of hourly medians plotted by time blocks on Fig. 6 appear quite similar, Table 3 indicates some seasonal effect in the long-term fading range. The range is larger during summer, and is also larger for the corner reflector at the higher elevation than for the dish. There is very little variation in the overall median values between time blocks, and the difference between the dish and the corner reflector appears to be slightly higher in summer.

2.3 Comparative Studies of Median Distributions

Although tropospheric scatter is not primarily involved in these experiments, it is of interest to compare first the measured distributions with theoretically expected values and with data from tropospheric scatter paths having similar path parameters. For this purpose, two hypothetical paths and the measured results obtained from two actual tropospheric scatter paths were used. The two hypothetical paths were considered to have the same antenna height as the actual path. One was assumed to have an angular distance which a tropospheric scatter path of the same length would have over a smooth earth, and

Table 3
Comparison of Winter and Summer Results

| | Overall Median, Decibels | | Difference of Overall Medians db | Long-Term Fading Range, Decibels (1% - 99%) | |
|----------------|--------------------------|---------------------|--|--|---------------------|
| Time Block No. | 3 m Dish | Corner Reflector | | 3 m Dish | Corner Reflector |
| <u>Winter:</u> | | | | | |
| 8 (0000-0600) | 198.4 | 193.2 | 5.2 | 8.9 | 14.8 |
| 1 (0600-1300) | 197.6 | 192.6 | 5.0 | 8.9 | 10.5 |
| 2 (1300-1800) | 198.3 | 192.8 | 5.5 | 12.4 | 14.0 |
| 3 (1800-2400) | 197.9 | 192.7 | 5.2 | 11.5 | 11.6 |
| <u>Summer:</u> | | | | | |
| 7 (0000-0600) | 198.1 | 192.7 | 5.4 | 13.5 | 16.2 |
| 4 (0600-1300) | 197.6 | 191.4 | 6.2 | 13.8 | 14.4 |
| 5 (1300-1800) | 197.3 | 189.9 | 7.4 | 11.4 | 10.7 |
| 6 (1800-2400) | 198.5 | 192.3 | 6.2 | 13.0 | 12.9 |

the other would have a path length corresponding to a smooth earth path having the same angular distance as the obstacle gain path. The actually measured paths were selected to correspond closely to these assumptions in path geometry and frequency. Table 4, below, shows the path constants used:

Table 4

Path Constants for Comparative Study

| | Path Distance, km | Angular Distance, Milliradians |
|-----------------------|-------------------------|--------------------------------------|
| Hypothetical Path A | 223 | 24.0 |
| Hypothetical Path B | 566 | 64.4 |
| Actual Paths: | | |
| Pikes Peak Obstacle | | |
| Gain (751 Mc) | 223 | 64.4 |
| Cheyenne Mt. -Garden | | |
| City (1046 Mc) | 364 | 26.7 |
| Cheyenne Mt. -Anthony | | |
| (1046 Mc) | 633 | 59.8 |

Overall time block medians and the long-term fading ranges for the hypothetical paths were determined from a consideration of the expected long-term variation of hourly medians. These distributions are obtained from the empirical $V(p, \theta)$ curves defined by Rice, et al,¹² which were determined from a large amount of experimental data representing a number of different geographical and climatic regions within the

United States. The time block medians and long-term fading ranges given there are measured relative to a calculated reference value of basic transmission loss, which is the median of all hourly median values in Time Block 2 (winter afternoon). The curves are assumed to be valid for all frequencies in the 70-4000 Mc range.

A comparison of the long-term fading range determined in this manner for the hypothetical paths with the ones measured on the Pikes Peak obstacle gain path is shown as Table 5 for all time blocks separately, for all hours during summer and winter, and for all hours of the year.

It is seen that the actually observed long-term fading ranges were considerably smaller than the ones predicted on the basis of scatter propagation, although the fading predicted for a scatter path having the same angular distance is a somewhat better estimate.

In order to provide a more valid basis for estimating long-term fading ranges and the distribution of hourly medians for knife-edge diffraction paths, use is made of a method suggested by K. A. Norton. The results of this method as applied to the Pikes Peak obstacle gain path will be compared with the actual measurements in what follows.

For the purpose of studying variations in hourly median field strength or transmission loss values a knife-edge diffraction path is considered to consist of two line-of-sight paths in tandem. The diffracting knife-edge constitutes a common

Table 5

Comparison of Hypothetical Tropospheric Propagation Paths Data with Measured Data from Pikes Peak Obstacle Gain Path

| Time Block | Long-Term Fading Range, db (1% - 99%) | | |
|-------------------|--|--|---|
| | Hypothetical Path A, 223 km, $\theta = 24$ miles | Hypothetical Path B, 566 km, $\theta = 64.4$ miles | Pikes Peak Obstacle Gain Path 223 km, $\theta = 64.4$ mi. (3 m Dish) |
| 8 (winter) | 42.1 | 21.1 | 8.9 |
| 1 | 37.6 | 13.9 | 8.9 |
| 2 | 32.9 | 14.0 | 12.4 |
| 3 | 39.2 | 16.3 | 11.5 |
| 7 (summer) | 42.2 | 21.4 | 13.5 |
| 4 | 37.7 | 28.1 | 13.8 |
| 5 | 25.1 | 18.2 | 11.4 |
| 6 | 36.5 | 19.0 | 13.0 |
| All Hours, Winter | 38.8 | 19.3 | 11.7 |
| All Hours, Summer | 41.9 | 26.0 | 13.4 |
| All Year | 39.7 | 26.4 | 14.3 |

terminal for the two paths. If the hourly median signal for each of the two line-of-sight paths is subject to random variations, V_1 and V_2 , then the random variation V expected on the mountain obstacle path would be $V = V_1 + V_2$, where V , V_1 and V_2 are random variables expressed in decibels. The resulting cumulative distribution of hourly medians for the entire path may be determined by the convolution of the distributions of V_1 and V_2 .¹³

The cumulative distributions of hourly medians for the two individual line-of-sight paths may be calculated by empirical formulas as functions of the path distance, the effective antenna heights, the carrier frequency, the horizon elevation angles, and season, summer or winter. The methods used are unpublished empirical methods communicated to the authors by P. L. Rice. This material will be described in detail in forthcoming NBS Technical Notes and in a U.S. Air Force Technical Order dealing with design procedures for tropospheric communication circuits. Results are shown on Fig. 7, where the empirical distributions are compared with the actually measured distributions. Comparison is made for the data on 751 Mc obtained using the 3-meter dish separately for all hours during the summer and during the winter months, and for the 100 Mc data for the summer months.

Calculation of the empirical distributions of hourly medians shown on Fig. 7 includes determination of the overall median reference value by Fresnel diffraction and ray optics methods which will be discussed in more detail in Section 3 below. What is primarily important here is the comparison of the slopes of the actually measured and the empirically predicted distribution curves shown on Fig. 7, rather than their absolute position on the basic transmission loss scale.

Table 6

Comparison of Actually Measured Fading Ranges with Empirical Predictions for Pikes Peak Obstacle Gain Path

| | Long-Term Fading Range in Decibels (1% - 99%) | |
|-------------------|---|----------------------|
| | Actually Measured | Empirical Prediction |
| <u>751 Mc</u> | | |
| All Hours, Winter | 11.7 | 11.5 |
| All Hours, Summer | 13.4 | 16.2 |
| <u>100 Mc</u> | | |
| All Hours, Summer | 7.0 | 9.0 |

The comparison of measured and predicted fading ranges from Fig. 7 is summarized in Table 6 below.

Table 6 shows that the empirical method just described provides much better estimates of the long-term fading range than the assumption of a tropospheric scatter path of the same linear or angular distance. This conclusion applies to this specific knife-edge diffraction path, and should be tested against data obtained from other knife-edge paths in order to arrive at an estimate of the uncertainty inherent in the prediction process. However, agreement of the predicted 1 - 99% long-term fading ranges is well within the sampling error of the empirical data on which this prediction is based and this suggests that the proposed method of predicting long-term fading ranges is a reliable one.

The data in Tables 5 and 6 have been plotted on Fig. 8 to obtain a better picture of the comparison between predicted and measured long-term fading ranges and their diurnal trends. As the empirical prediction method just mentioned does not distinguish between individual time blocks, it is represented by a straight line for all summer and winter time blocks, respectively. In spite of the large discrepancy between the measured fading ranges and the ones predicted on the basis of scatter propagation, it is of interest to note that the predicted diurnal trend is evident in the measured data for the summer time blocks, although to a considerably lesser degree. This is not the case for the winter time blocks due to the relatively large measured Time Block 2 long-term fading range.

An additional comparison of the measurement results was made with similar data obtained from two actually measured tropospheric propagation paths which represent a geographical location similar to the Pikes Peak obstacle gain path. In addition thereto, these paths correspond most closely to the hypothetical paths described above in path distance and angular distance, and at the same time, represent a similar carrier frequency. The hourly median distributions for these two paths were taken from unpublished reports. A description of the paths and the various experiments conducted are contained in a National Bureau of Standards Circular.¹⁴

Fig. 9 compares the distribution of hourly medians measured during the summer months over the Pikes Peak obstacle gain path with the two paths between Cheyenne Mountain and points in the eastern plains. It is seen that the long-term fading range is smallest for the obstacle gain path;

Table 7

Comparison of Long Tropospheric Propagation Path Results

| Path | Frequency Mc | Time Period | No. of Hours | Basic Transmission Loss Overall Median db | Long-Term Fading Range, db (1% - 99%) |
|-------------------------------|-----------------|------------------------------|-----------------|---|---|
| Pikes Peak Obstacle Gain | 751 | Summer 1960 | 613 | 198.7 | 13.4 |
| Cheyenne Mt. - Garden City | 1046 | Summer 1952 | 1646 | 208.9 | 30.5 |
| Cheyenne Mt. - Anthony | 1046 | Summer 1952 (July-August) | 184 | 225.5 | 21.5 |

it is quite large for the Garden City path which represents the same linear path distance, and slightly larger for the Anthony path which represents the same angular distance, but a substantially greater linear path distance. Table 7 shows the comparison of overall median values and ranges taken from Fig. 9

The overall medians have been added for completeness of the information. It is quite clear that transmission loss tends to be smaller for a knife-edge diffraction path as compared to tropospheric scatter paths of similar length. Perhaps even more significant is the substantial reduction in the long term fading range. Although there are fewer hours of measurements available for the Cheyenne Mountain-Anthony path, Table 6 shows that a tropospheric scatter path of comparable linear distance has a substantially greater long-term fading range than an obstacle gain path, whereas a scatter path of similar angular distance has only a moderately greater long-term fading range. This agrees well with the results obtained by the application of empirical methods for determining fading range--the method based on scatter propagation paths yielding substantially greater fading ranges than the method based on line-of-sight paths.

2.4 Frequency Dependence of the Distributions of Hourly Medians

Fig. 10 shows a comparison of all measured data on 100 Mc and 751 Mc during the two weekly periods when the receiver site on Pikes Peak was operated. These are overall summer-time distributions; they have not been separated into time blocks because of the comparatively few hours available. As expected, the long-term fading range is smaller for the line-of-sight path to the top of the peak than for the obstacle gain path. Overall median and ranges for this period are given in Table 8.

Table 8

Data from Distributions of Hourly Medians

| Path and Frequency | Basic Transmission Loss Overall Median, db | Long-Term Fading Range, db (1%-99%) |
|---------------------------------------|---|--|
| Beulah-Pikes Peak, 100 Mc | 128.2 | 5.7 |
| Beulah-Pikes Peak, 751 Mc | 132.0 | 6.3 |
| Beulah-Table Mesa, 100 Mc | 165.3 | 7.0 |
| Beulah-Table Mesa, 751 Mc (Dish) | 197.0 | 13.0 |
| Beulah-Table Mesa, 751 Mc (Corner) | 191.6 | 14.7 |

This tabulation shows a substantial frequency dependence of the fading range for the obstacle gain path--more than doubled when comparing 100 Mc with either one of the 751 Mc antennas. There is not nearly that much frequency dependence on the line-of-sight path. It has already been shown that the $V(p, \theta)$ distributions are not appropriate for use in predicting the performance of knife-edge diffraction paths, and that much better agreement is obtained by the use of a different empirical method taking into account carrier frequency and horizon elevation angles.

3. Height Gain Studies

Previous measurements made of obstacle diffraction over Pikes Peak³ showed marked agreement between the predicted and observed variation of transmission loss with height. These measurements were made using a shorter path and with a relatively smooth terrain area in the immediate foreground of the antenna whose height was varied.

The 751 Mc equipment installed on Table Mesa permitted the collection of similar data for antenna heights up to 100 feet using a telescopic tower with dual receivers and recorders. However, the Table Mesa site differs from the receiving site previously used in that the terrain is very rough except for a small flat area immediately in front of the receiver site, which is only large enough for approximately one-third of the first-Fresnel-zone ellipse. It has been previously shown that the cumulative distributions of hourly basic transmission loss medians for the two antenna heights on 751 Mc have approximately the same dispersion and the medians are separated by approximately 5 db in winter, and up to 7.4 db in summer. Using a small stored-program electronic computer the height distribution of field strength or basic transmission loss was calculated by methods of geometrical optics using the vector sum of four rays.^{2, 7} Each of the rays has a magnitude and phase value determined by reflections from the ground and diffraction by the knife-edge type obstacle. The reflecting planes were assumed to be parallel to a smooth earth's surface, and to pass through the bases of the antenna towers. Reflection coefficients of 0.5 and 0.9 were assumed, with a phase shift of 180 degrees occurring at the reflecting planes. The attenuation and phase-shift at the obstacle were calculated using the asymptotic expansions for Fresnel integrals.¹ This was justified due to the magnitude of the parameters involved. For all calculations a refractivity value $N_s = 290$ was assumed, which corresponds to average winter afternoon for the geographical region where the measurements were made. Changes in the N_s value within the range 240 to 320 N-units did not materially affect the relative height dependence of basic transmission loss.

A height-gain run was performed in the morning hours of March 25, 1960. For each position of the corner reflector antenna (mounted on the telescopic tower) the basic transmission loss was determined for both receiving antennas, so that the values measured could be corrected for changes recorded on the fixed antennas. The results are plotted versus receiving antenna height on the subsequent figures in order to permit comparison with calculated values using various parameters.

Fig. 11 shows the comparison of the measured height dependence with calculated values, using reflection coefficients of 0.9 and 0.5. There is no agreement in the magnitude of the transmission loss or in the number of lobes. The measured data show only one lobe with a maximum at approximately 21 meters above ground,

whereas the theoretical calculations predict four to five lobes within the height interval measured. A change in the reflection coefficient only changes the magnitude of the maxima and minima. Similarly, any change in the assumed elevation of the transmitting antenna has little or no effect upon the position and number of lobes at the receiver, but can modify the transmission loss approximately the same amount at all heights. Height-gain experiments using the transmitting antenna were not performed.

Studies were also made assuming the cross section along the profile of the refracting knife-edge to be rounded. The terrain profile cross section through the top of Pikes Peak can be approximated by a circular arc with a radius of roughly 11.5 kilometers. Following, in general, the procedure given by Wait and Conda,¹⁵ the resultant diffracted field as a function of receiving antenna height was calculated again as the vector sum of four rays, each of which is affected by the rounded obstacle and by reflections from the terrain in the foreground of the antennas. These results are shown on Fig. 12, together with the measured height-gain run and the theoretical curve for the ideal knife-edge. Both theoretical curves are based on a reflection coefficient of 0.9. It is seen that only the absolute values of transmission loss are affected by "rounding" the knife-edge; the number and position of the lobes with antenna height remains the same. Additional calculations show that the change in transmission loss depends on the radius of curvature assumed; as this is somewhat arbitrary for this terrain configuration, the assumption of 11.5 km depends on how much of the profile the arc is fitted to.

Fig. 11 shows that the long-term median values of transmission loss observed on the dish at 8.2 meters and the corner reflector at 16.5 meters have approximately the same difference as is indicated by the measured height gain curve. For the two different heights used for the higher antenna (corner reflector at 16.5 and 22.3 meters) there is little difference in the values of transmission loss observed. This tends to confirm the similarity of long-term transmission loss values observed at the two heights as shown in Fig. 5.

It is quite clear from the above discussion that the basic transmission loss dependence on antenna height cannot be represented in this case by the simple four-ray knife-edge model, even if the knife edge is assumed to be rounded. The reason becomes evident if the transverse profile through the obstacle is studied, which is a terrain profile drawn through the obstacle at right angles

to the propagation path. Fig. 13 is a photograph of the visual horizon as seen from the transmitting antenna with various visible ridge lines emphasized. A grid is superimposed which shows the angles subtended from the transmitting site. It is seen that the transmitting antenna beam, with a 7.7° half-power beam width sees a substantial portion of the ridge line on either side of the principal obstacle. Similar conditions exist if the transverse profile is viewed from the receiving terminal. Thus field contributions may exist from the ridges and other terrain features between the terminals and Pikes Peak illuminated by the antenna beams. It has so far not been possible to make a quantitative study of these contributions in order to use them for field computations.

4. Vertical Space Diversity and Fading Characteristics

A detailed study of the short-term fading characteristics observed on this path is contained in another paper.¹⁶ A number of possible mechanisms appear responsible for the fading. These include those associated with prolonged space-wave fadeouts, which resemble phenomena observed on within-the-horizon paths, as well as those associated with scattering components. Other mechanisms appear to be due to the terrain configuration and may be the cause of an intermediate type of fading, characterized by fadeouts on the order of 5 db which last less than a few minutes.

In view of the apparent positive correlation between the 751 Mc signals recorded simultaneously on the two receiving antennas, studies were

performed to determine the correlation coefficient between instantaneous envelope values for various sample periods. For this purpose, the transmission loss information recorded on magnetic tape was digitized and fed into a computer program. The tape contained adequate timing signals to insure proper evaluation without time lag. Table 9, below, contains the time and duration of each sample, the separation of the receiving antennas, and the resulting correlation coefficient. For purpose of digitizing, the magnetic tape was sampled once per second. The correlation coefficients listed apply to basic transmission loss in decibels; a check revealed that results were not materially different if receiver input voltages (proportional to field strength) were correlated.

The samples were picked to represent different types of the signal as it appeared on the visual recording charts for the two antennas. They are not to be considered taken at random in a statistical sense; therefore they serve only to illustrate the phenomenon, and cannot be used to establish a time or spacing dependence, or similar results. They show, however, that moderately high correlation exists between simultaneous envelope values of the signal received on vertically spaced antennas, and that the correlation coefficient seems to be higher at nighttime and for closer spaced antennas, and that these results make the effectiveness of vertical space diversity questionable for a path of this type. A more complete analysis using many more samples evenly distributed over the recording period would be necessary to draw final conclusions on the diurnal variation and other characteristics of the correlation coefficient.

Table 9
Results of Envelope Correlation Studies for Pikes Peak Obstacle Gain Path

| Date and Time of Sample (all in 1960) | Length, Minutes | Antenna Spacing, Meters | Correlation Coefficient |
|--|--------------------|----------------------------|----------------------------|
| June 13, 1745-1800 | 15 | 14.1 | 0.491 |
| June 13, 2120-2125 | 5 | 14.1 | 0.503 |
| June 13, 2200-2220 | 20 | 14.1 | 0.625 |
| June 14, 1010-1020 | 20 | 14.1 | 0.204 |
| June 15, 0738-0748 | 10 | 14.1 | 0.242 |
| June 15, 1200-1210 | 10 | 14.1 | 0.033 |
| June 15, 1800-1805 | 5 | 14.1 | 0.537 |
| June 16, 0350-0400 | 10 | 14.1 | 0.656 |
| September 15, 1700-1710 | 10 | 8.3 | 0.555 |
| September 15, 1920-1930 | 10 | 8.3 | 0.677 |
| September 15, 2126-2146 | 20 | 8.3 | 0.685 |
| September 16, 0255-0305 | 10 | 8.3 | 0.331 |
| September 16, 1015-1025 | 10 | 8.3 | 0.780 |
| September 16, 1120-1130 | 10 | 8.3 | 0.450 |

A visual representation of the instantaneous envelope correlation may be obtained by applying the tape-recorded signals to an x - y plotter. Fig. 14 shows two such samples, and a good qualitative idea of the magnitude of the correlation coefficient may be obtained thereby.

Fig. 15 shows examples of the correlation coefficient between hourly median values of basic transmission loss. In general, hourly medians tend to be more highly correlated than instantaneous values. The two graphs shown represent the two antenna separations used. The correlation coefficient is substantially higher for the closer spaced antennas (8.3 m). It cannot be determined, however, if this is entirely due to the spacing, as the two samples were taken at different times. The graphs indicate the antenna spacing, the number of hours, the standard deviations of hourly medians for each antenna, and the correlation coefficient. Hourly medians determined with the 3 m dish are plotted along the y-axis, whereas the corner reflector data are plotted along the x-axis.

Finally, a new analysis of fade durations and signal distributions is shown on Fig. 16. Four periods of record ranging from 6 hours to more than 200 hours each were analyzed to determine the distribution of fades as well as high signal of various levels and duration periods. Each curve shown corresponds to one of these levels, and the points plotted are the percentages of the total time the signal remained either above or below the indicated level for the duration given by the ordinate. The median is the dividing line; for each graph curves to the left of the median represent fades, and the ones to the right represent periods of signal higher than the median. The asymptotic extensions of the curves toward a zero fade or signal duration become the distribution of instantaneous signal levels for each period in the limit. As an example, in the upper right hand graph (period August 8-12), the curve labelled "202" indicates the distribution of durations when the basic transmission loss exceeded 202 db: 1% of all "fades" to 202 db was of at least 8 minutes duration.

This type of representation permits an analysis of fades or short-term variations in terms of basic transmission loss levels, which may be easily related to any arbitrary reference, like the overall median of the period considered. This type of presentation can be used to determine, at least statistically, the characteristics of individual fades. For example it might be of interest to know how many fades occurred whose duration was between one and two minutes. The difference between the percentage of the total time the signal

fell below the specified level for durations of one and two minutes respectively can be read from this type of presentation. From this information the number of fades within this range of duration can easily be determined for the entire period of the analysis.

5. Conclusions

The analysis of 751 Mc data from a long obstacle gain path showed principally that the distribution of hourly medians of field strength or basic transmission loss may be approximated by the convolution of cumulative distributions for two line-of-sight paths in tandem which have the obstacle as a common terminal. As expected, these long-term fading characteristics are quite different from the ones observed for tropospheric scatter propagation over comparable distances. No significant diurnal variation in propagation characteristics was observed on the obstacle-gain path, and the indication is that seasonal variations are small. Due to the limited width of the obstacle, the knife-edge approximation by a semi-infinite plane, or half-cylinder may not be entirely appropriate, although a somewhat arbitrary assumption of curvature leads to theoretical values of transmission loss equivalent to observed values.

Correlation studies of the signal received on vertically spaced antennas suggest that space diversity may not be very effective on circuits utilizing obstacle gain. Transmission loss recordings show slow and deep fades occurring simultaneously on antennas vertically separated 14.1 and 8.8 meters. Correlation was somewhat lower for the greater spacing.

It is hoped that additional diversity experiments can be performed using this path with the antennas spaced horizontally in line with and normal to the path profile.

The outstanding advantages of obstacle gain paths of this type are that the signal level is significantly higher than expected for scatter paths of comparable length, and the amplitude of rapid Raleigh-fading components is substantially reduced. However, the received field strength is lower than values calculated using the idealized knife-edge theory. This is probably due to the profile through the obstacle, which represents a rounded knife-edge, and to reflections and contributions from other terrain features.

These and similar measurements show that relatively high signal strengths are consistently observed behind mountain ridges. Thus it is unlikely that mountain ranges can always be relied upon to shield potential interference. Special

consideration to this phenomena should be given in locating radio astronomy or space communication terminals.

6. Acknowledgements

The authors wish to thank all the personnel of the Propagation-Terrain Effects Section who contributed to the installation and operation of the equipment, and the collection and the analysis of the data, and to Messrs. K. A. Norton and G. W. Haydon for their review and suggestions. Transmission loss calculations for a "rounded" knife-edge were performed by Messrs. H. T. Dougherty and L. J. Maloney. Drafting work was performed by J. C. Harman and his group, and the manuscript was typed by Mrs. D. J. Hunt.

7. Table of References

1. J. C. Schelleng, C. R. Burrows and E. B. Ferrell, "Ultra short-wave propagation," *Proc. IRE*, 21, pp. 427-463; March, 1933.
2. F. H. Dickson, J. J. Egli, J. W. Herbstreit, and G. S. Wickizer, "Large reductions of VHF transmission loss and fading by the presence of a mountain obstacle in beyond-line-of-sight paths," *Proc. IRE*, 41, pp. 967-969; August, 1953. See also subsequent correspondence by Crysdale, and rebuttal by Dickson, et al, in *Proc. IRE*, 43, pp. 627-628; May, 1955.
3. R. S. Kirby, H. T. Dougherty, and P. L. McQuate, "Obstacle gain measurements over Pikes Peak at 60 to 1046 Mc," *Proc. IRE*, 43, pp. 1467-1472; October, 1955. This paper contains an extensive list of references to previous work.
4. T. Kono and M. Hirai, "Use of diffraction effect of mountains for VHF radio communication," *Journal of the Radio Research Laboratories (Japan)*, 2, pp. 293-309; July, 1955.
5. K. Nishikori, Y. Kurihara, M. Fukushima, and M. Ikeda, "Broad and narrow beam investigations of SHF diffraction by mountain ridges," *Journal of the Radio Research Laboratories (Japan)*, 4, pp. 407-422; October, 1957.
6. M. Hirai, Y. Fujii, and H. Saito, "An experimental investigation of the diffraction at VHF and UHF by mountain ridges," *Journal of the Radio Research Laboratories (Japan)*, 5, pp. 189-211; July, 1958.
7. J. M. Crysdale, J. W. B. Day, W. S. Cook, M. E. Psutka, and P. E. Robillard, "An experimental investigation of the diffraction of electromagnetic waves by a dominating ridge," *IRE Trans. on Antennas and Propagation*, AP-5, pp. 203-210; April, 1957. See also subsequent discussion by Crysdale in AP-6, pp. 293-295; July, 1958.
8. K. Kakita, F. Iwai, and S. Ieiri, "Radio transmission beyond line-of-sight between Kyushu and Anami-Oshima Island," *Electrical Communication Laboratory Journal*, N.T.T. (Japan), 8, pp. 1183-1213; 1959.
9. Private communication from Western Electric Co.
10. B. R. Bean, "Prolonged space-wave fadeouts at 1046 Mc observed in Cheyenne Mountain propagation program," *Proc. IRE*, 42, pp. 848-853; May, 1954.
11. K. A. Norton, P. L. Rice, and L. E. Vogler, "The use of angular distance in estimating transmission loss and fading range for propagation through a turbulent atmosphere over irregular terrain," *Proc. IRE*, 43, pp. 1488-1526; October, 1955.
12. P. L. Rice, A. G. Longley, and K. A. Norton, "Prediction of the cumulative distribution with time of ground wave and tropospheric wave transmission loss; Part I - The prediction formula," *NBS Technical Note No. 15*; July, 1959.
13. W. B. Davenport, Jr., and W. L. Root, "An introduction to the theory of random signals and noise," McGraw-Hill Book Co., Inc., New York, 1958. See Chapter 3, pp. 35-37.
14. A. P. Barsis, J. W. Herbstreit, and K. O. Hornberg, "Cheyenne Mountain tropospheric propagation experiments," *NBS Circular* 554; January, 1955.
15. J. R. Wait and A. M. Conda, "Diffraction of electromagnetic waves by smooth obstacles for grazing angles," *NBS Journal of Research*, 63-D, pp. 181-197; September-October, 1959.
16. A. P. Barsis and M. E. Johnson, "Prolonged space-wave fadeouts in tropospheric propagation," *NBS Technical Note No. 88*; February, 1961.

OUTLINE MAP FOR BEULAH-TABLE MESA PROPAGATION PATH (COLORADO)

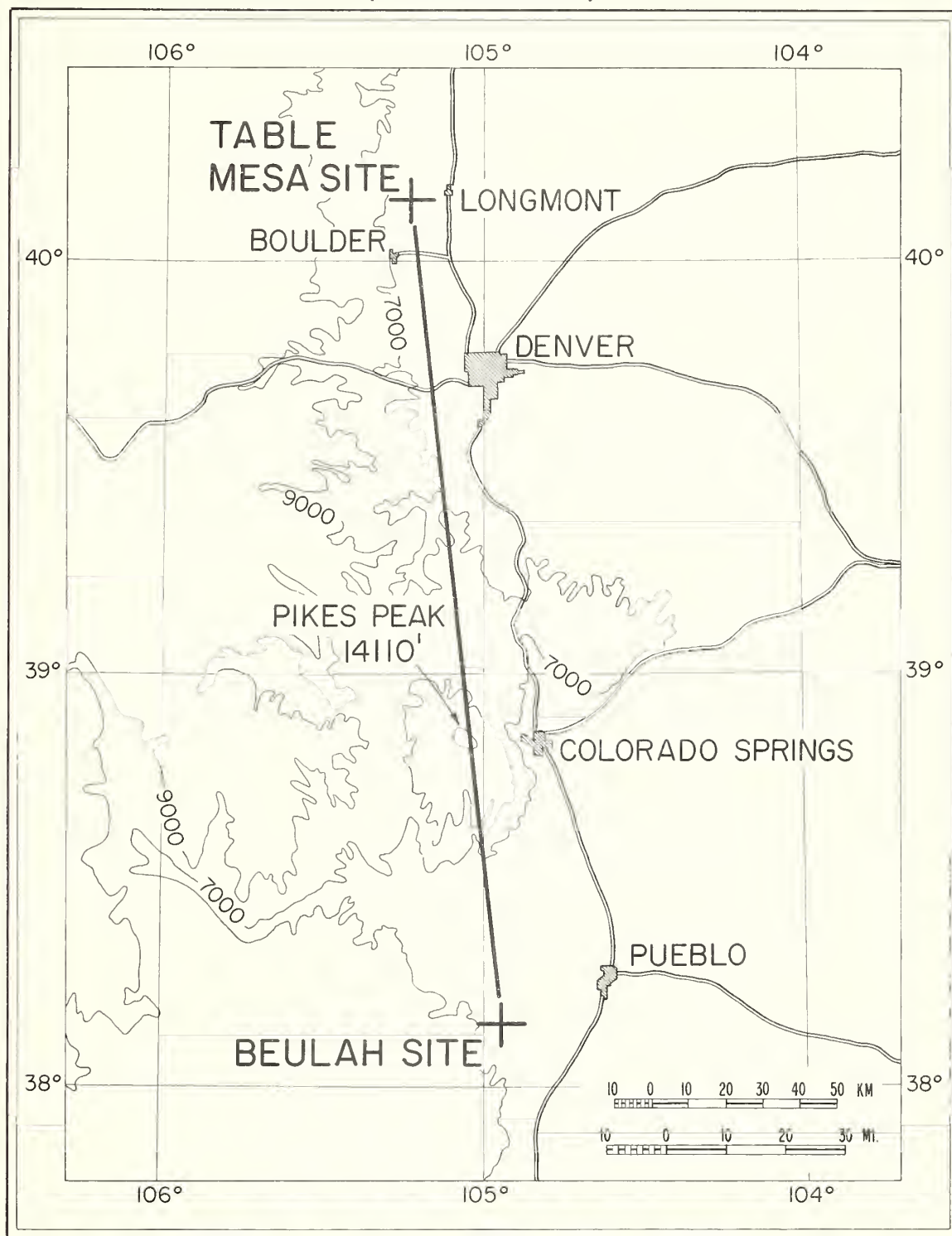


Figure 1

TERRAIN PROFILE OF COLORADO OBSTACLE GAIN PATH

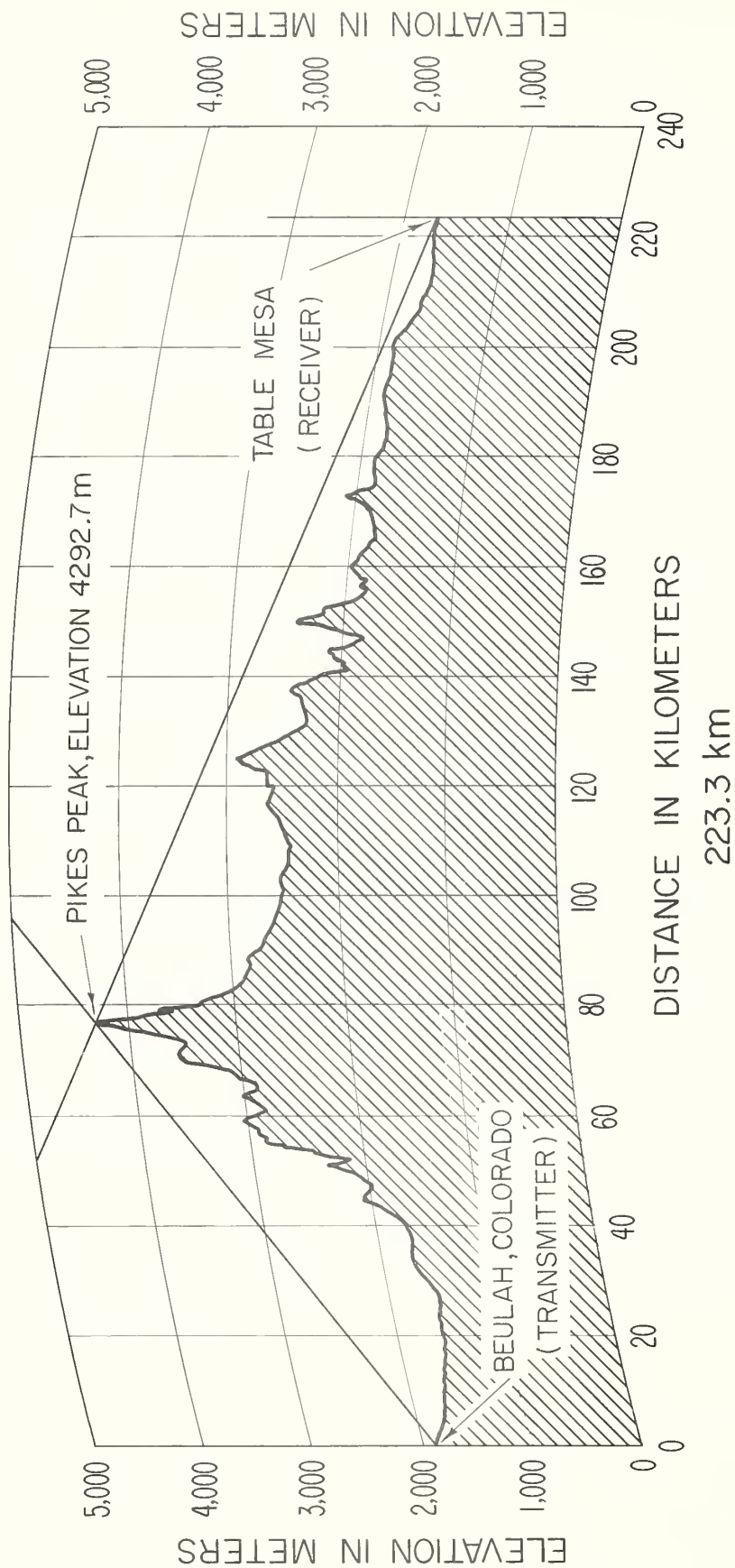


Figure 2

SIMULTANEOUS CHART RECORDINGS OF KNIFE EDGE AND LINE OF SITE PROPAGATION BEULAH TO TABLE MESA AND PIKES PEAK AUGUST 10, 1960

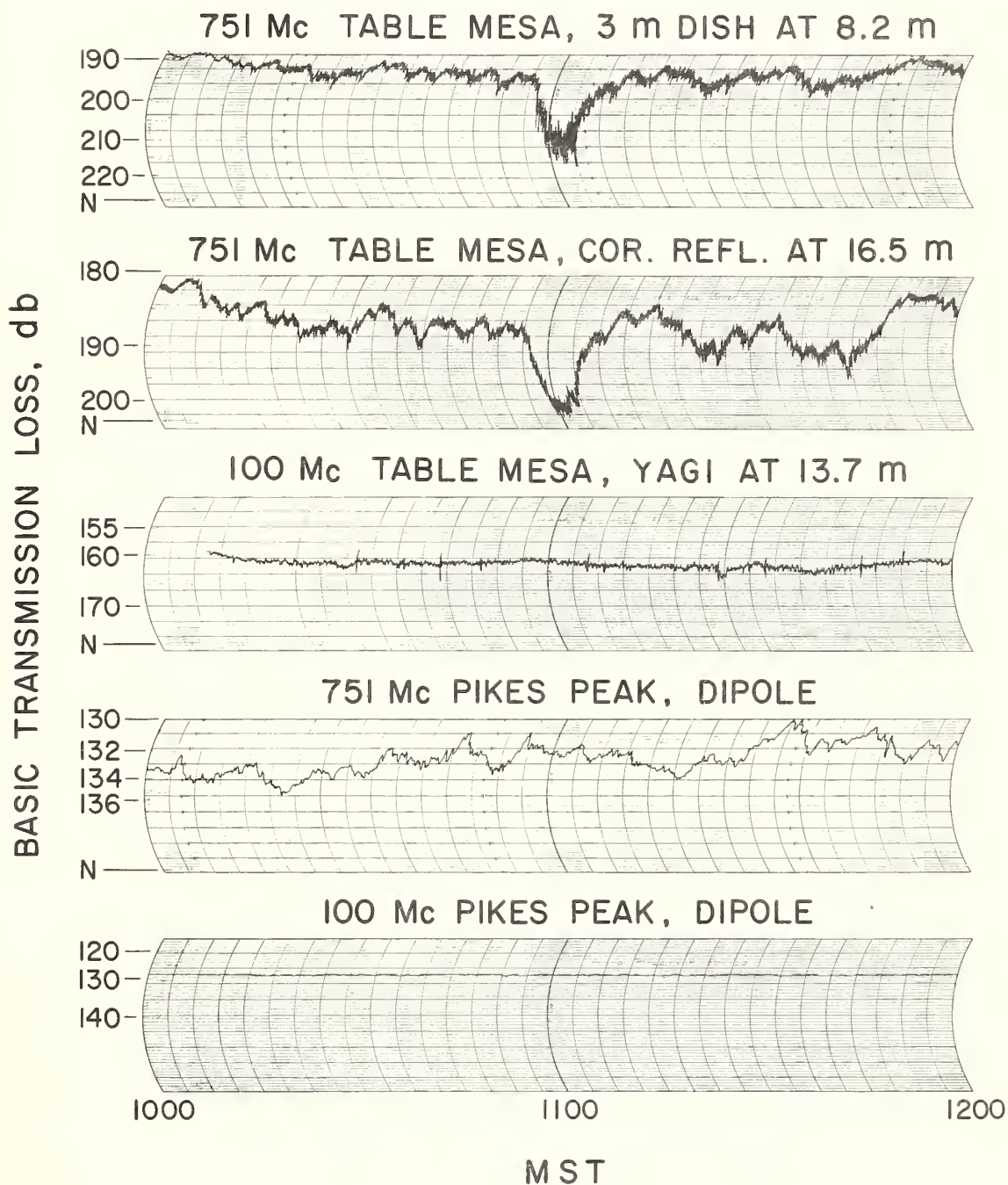


Figure 3

DAY TO DAY VARIATION IN HOURLY MEDIAN LEVELS BY HOUR OF THE DAY AUGUST 8-12, 1960

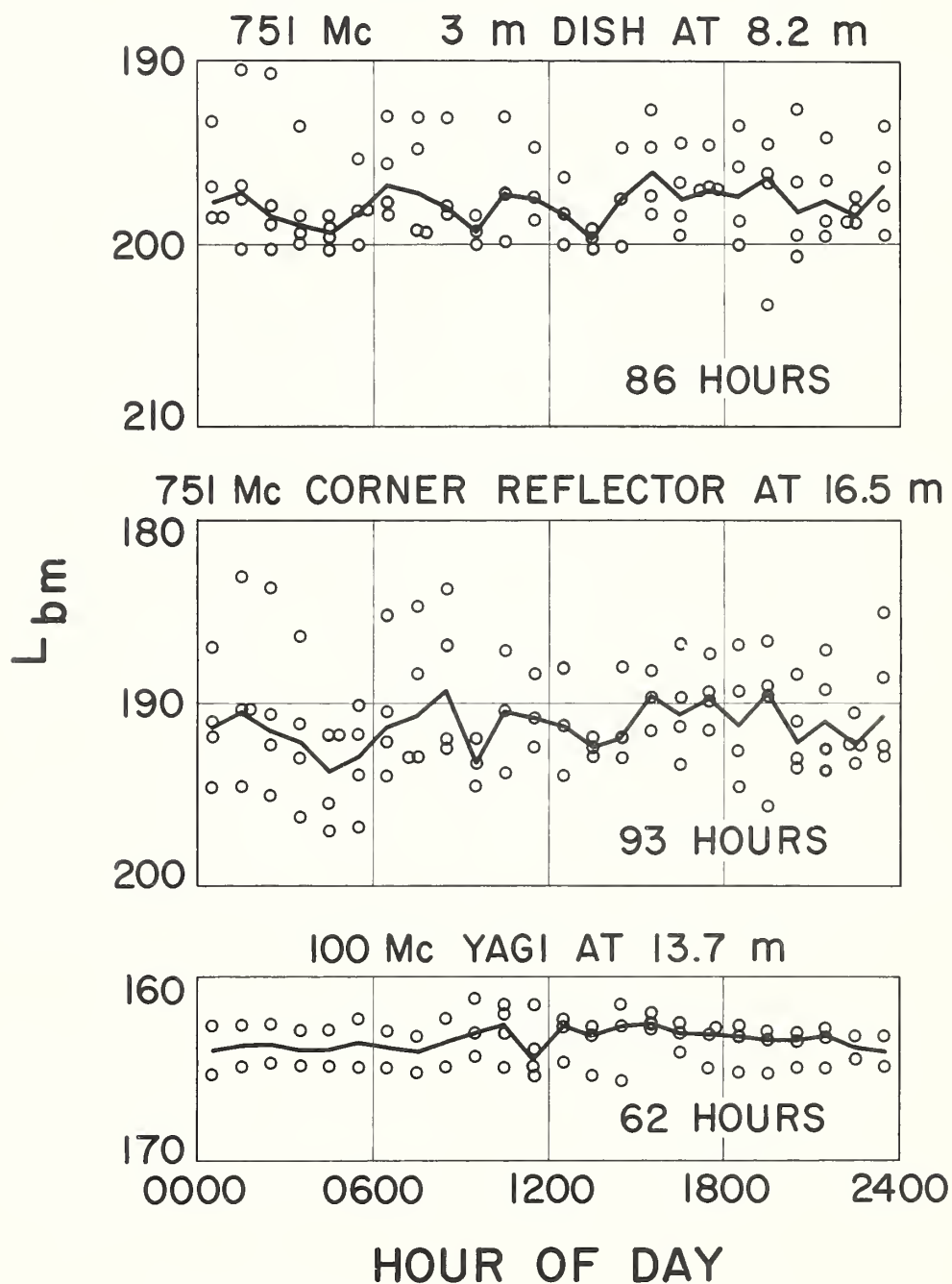


Figure 4

SEASONAL TREND OF OVERALL WEEKLY MEDIANS BEULAH - TABLE MESA PATH 751 MC

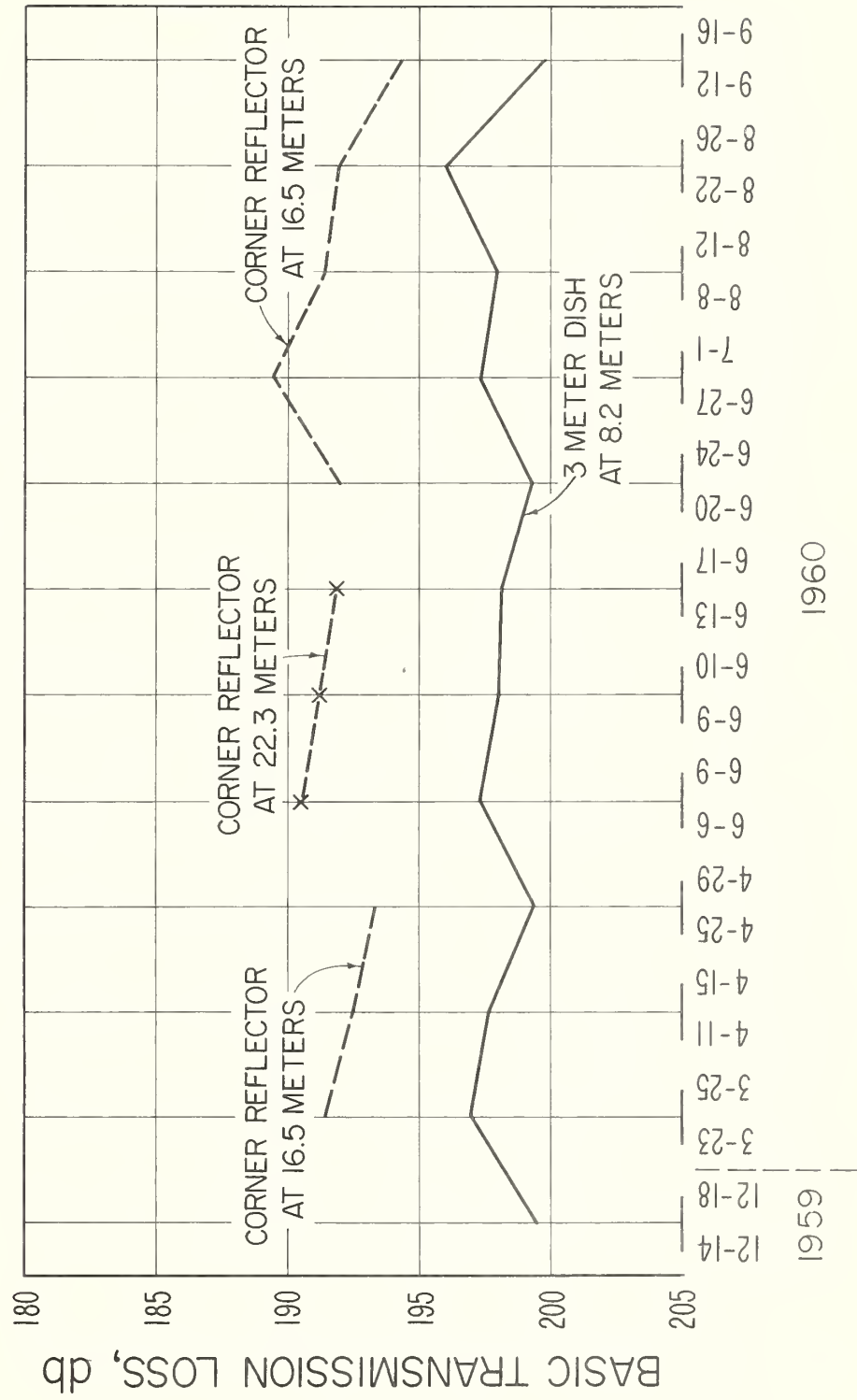


Figure 5

DISTRIBUTIONS OF HOURLY MEDIAN BASIC TRANSMISSION LOSS VALUES PIKES PEAK OBSTACLE GAIN PATH 751 MC

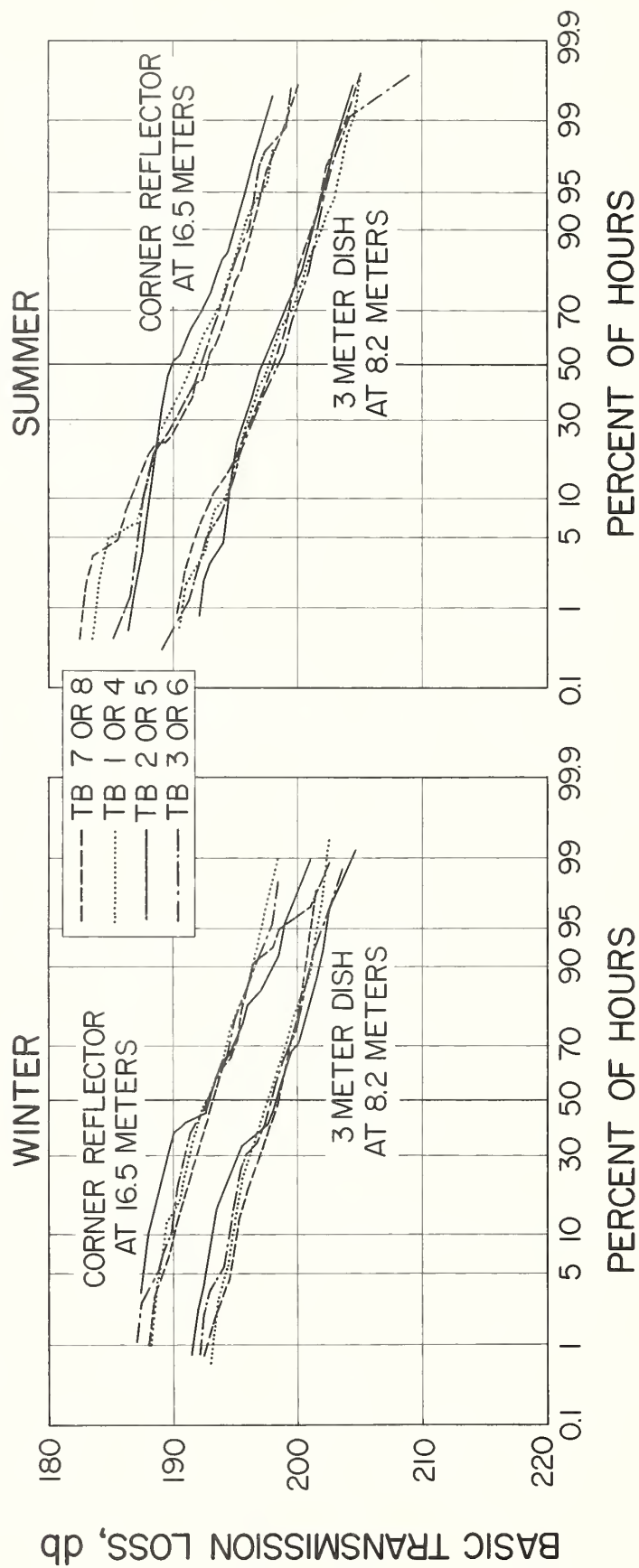


Figure 6

PREDICTED AND MEASURED CUMULATIVE DISTRIBUTIONS
OF BASIC TRANSMISSION LOSS HOURLY MEDIANS
PIKES PEAK OBSTACLE GAIN PATH

DECEMBER 1959 — SEPTEMBER 1960

----- PREDICTED DISTRIBUTION
————— MEASURED DISTRIBUTION

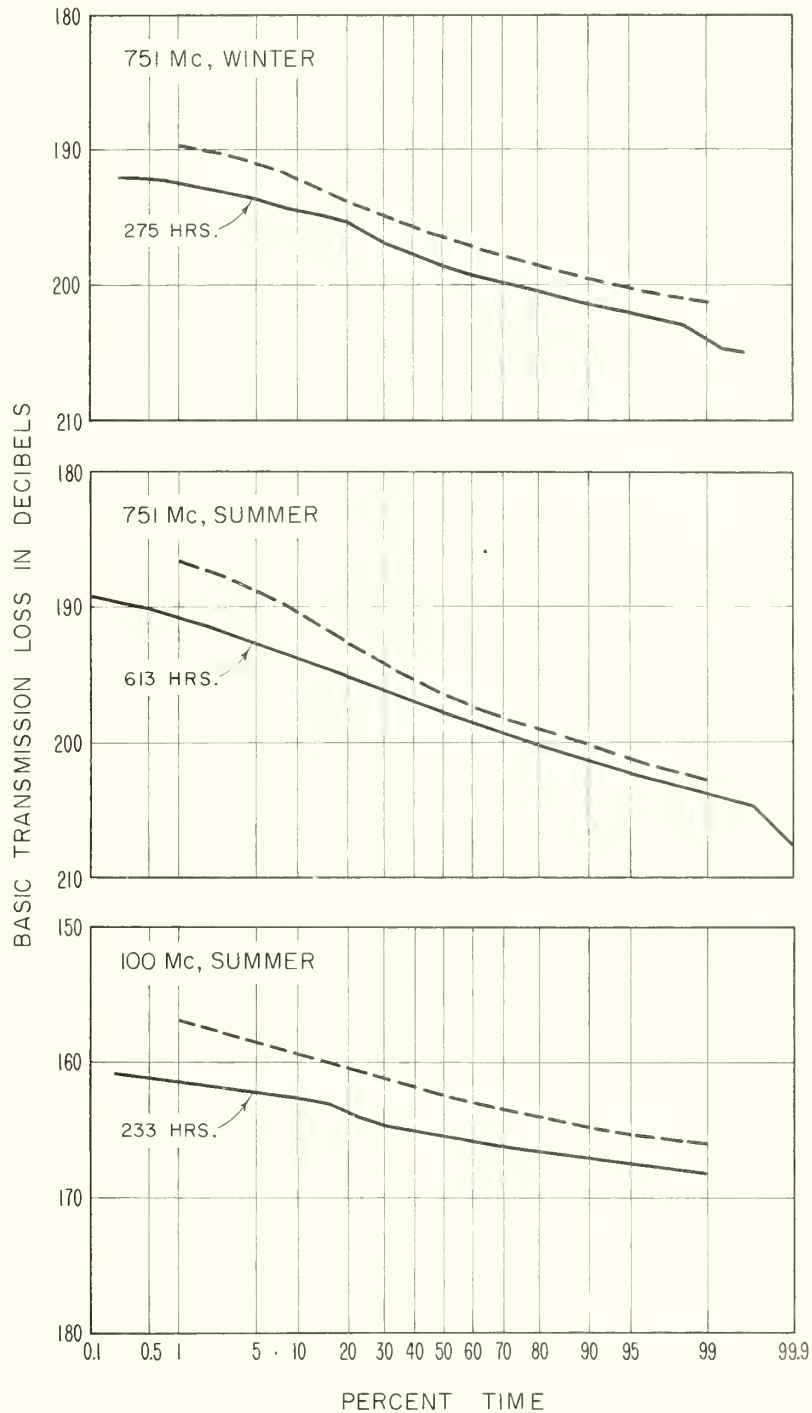


Figure 7

COMPARISON OF PREDICTED AND MEASURED DIURNAL AND SEASONAL VARIATIONS OF THE LONG-TERM FADING RANGE

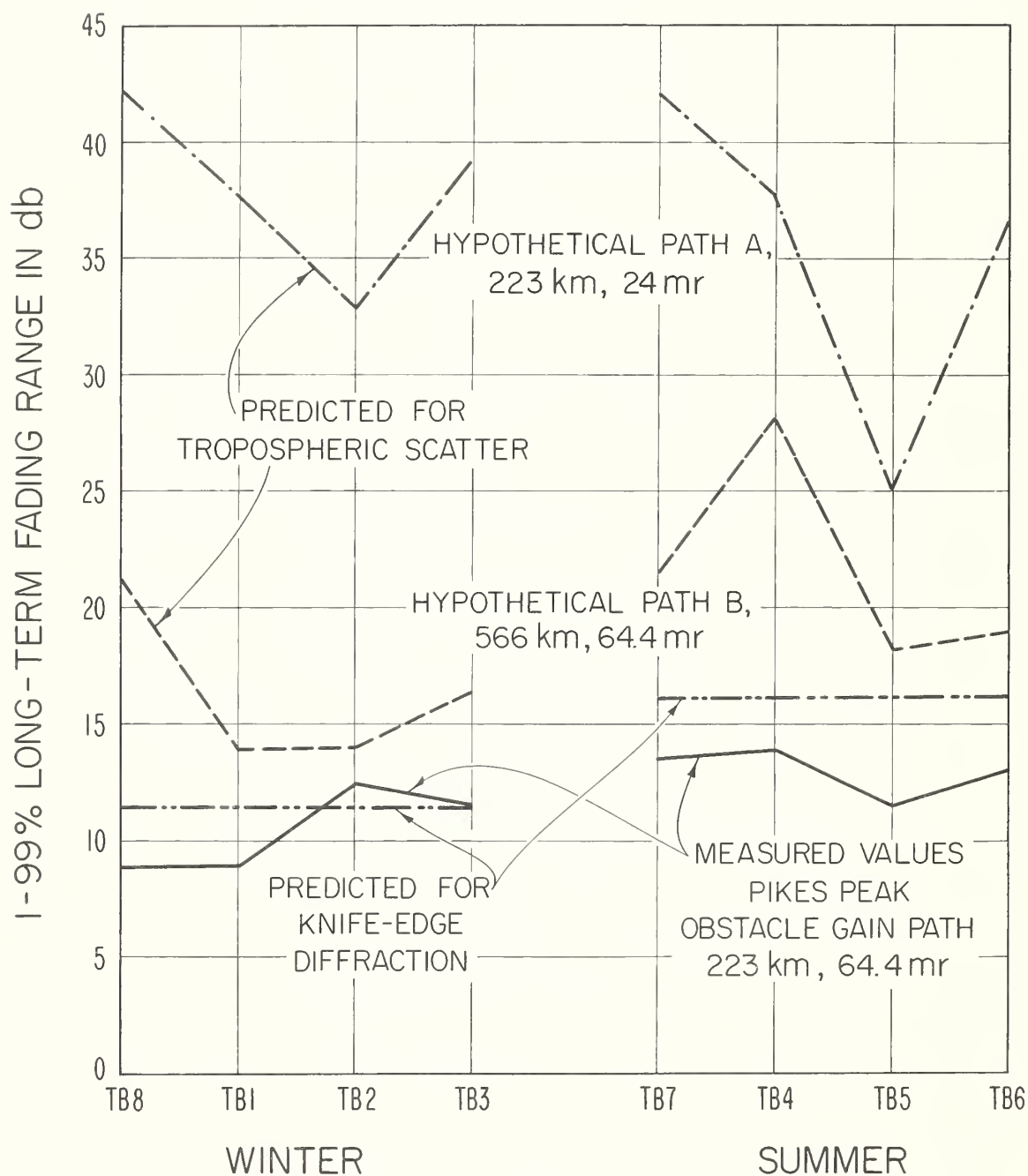


Figure 8

CUMULATIVE DISTRIBUTIONS OF HOURLY MEDIAN BASIC TRANSMISSION LOSS VALUES ALL HOURS, SUMMER COLORADO-KANSAS PATHS

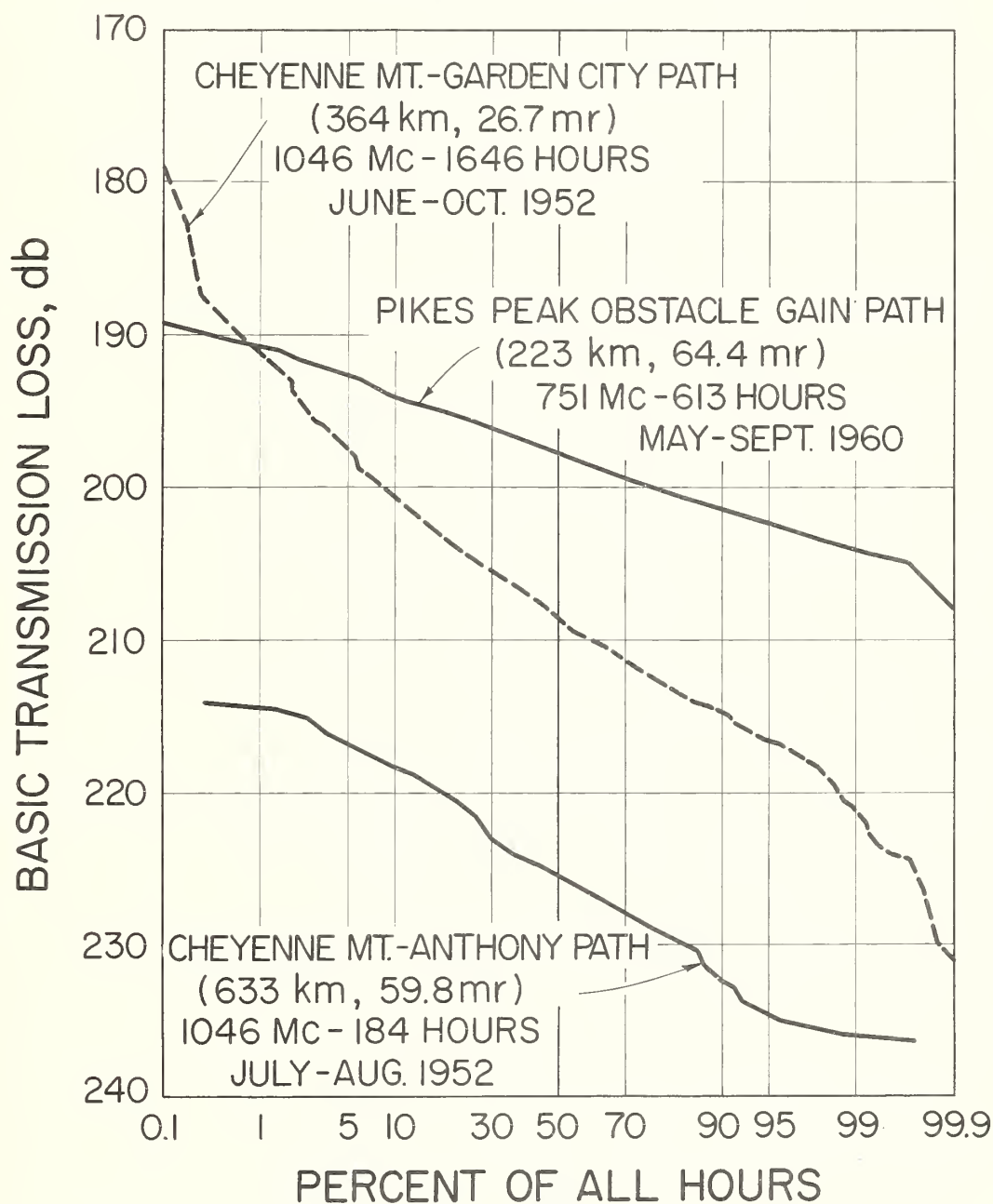


Figure 9

MEASURED DISTRIBUTIONS OF HOURLY MEDIANS BASIC TRANSMISSION LOSS VALUES AUGUST 8-12 AND 22-26, 1960

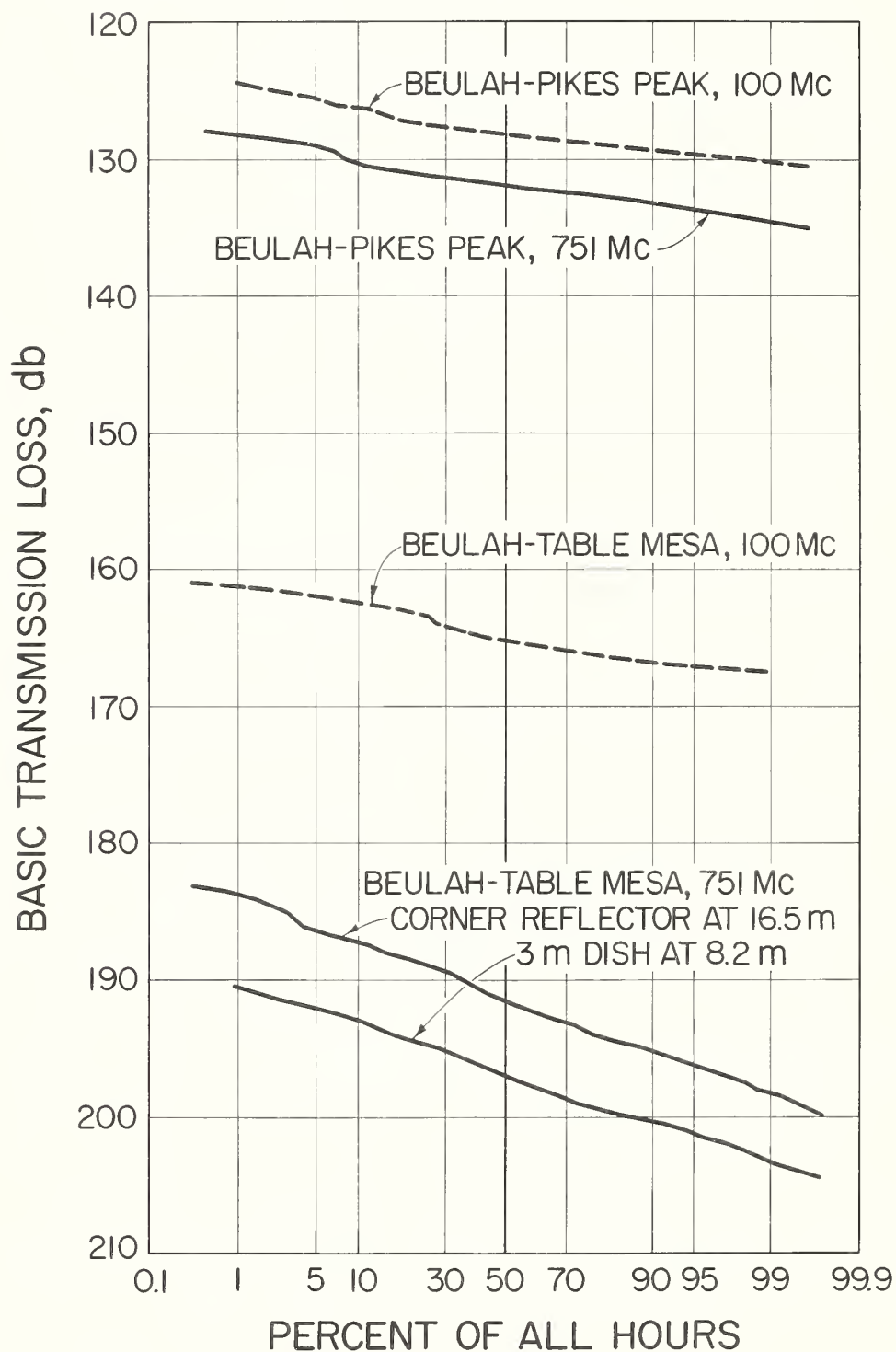


Figure 10

COMPARISON OF CALCULATED AND MEASURED HEIGHT - GAIN CURVES PIKES PEAK OBSTACLE GAIN PATH

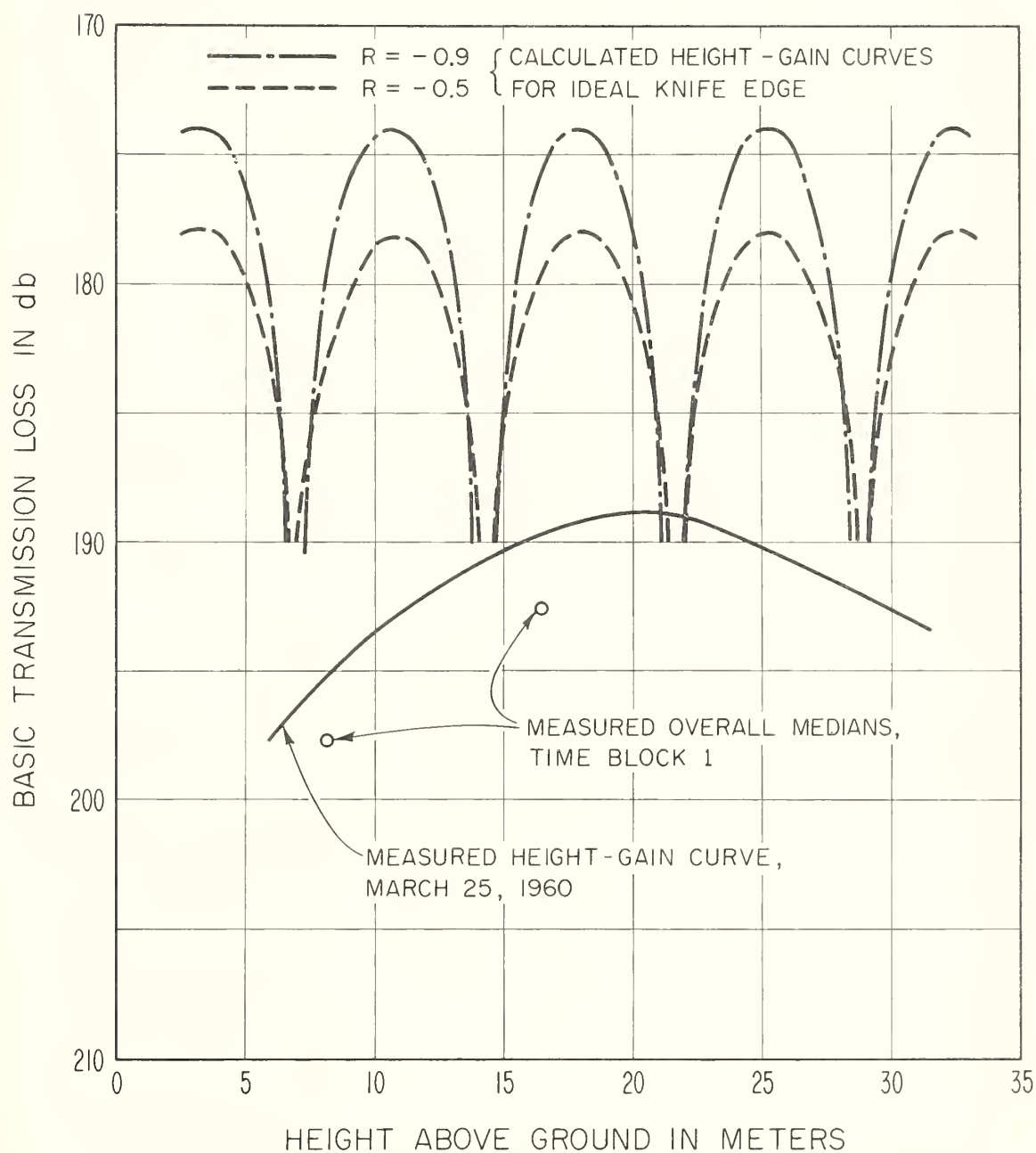


Figure II

COMPARISON OF CALCULATED AND MEASURED HEIGHT - GAIN CURVES PIKES PEAK OBSTACLE GAIN PATH

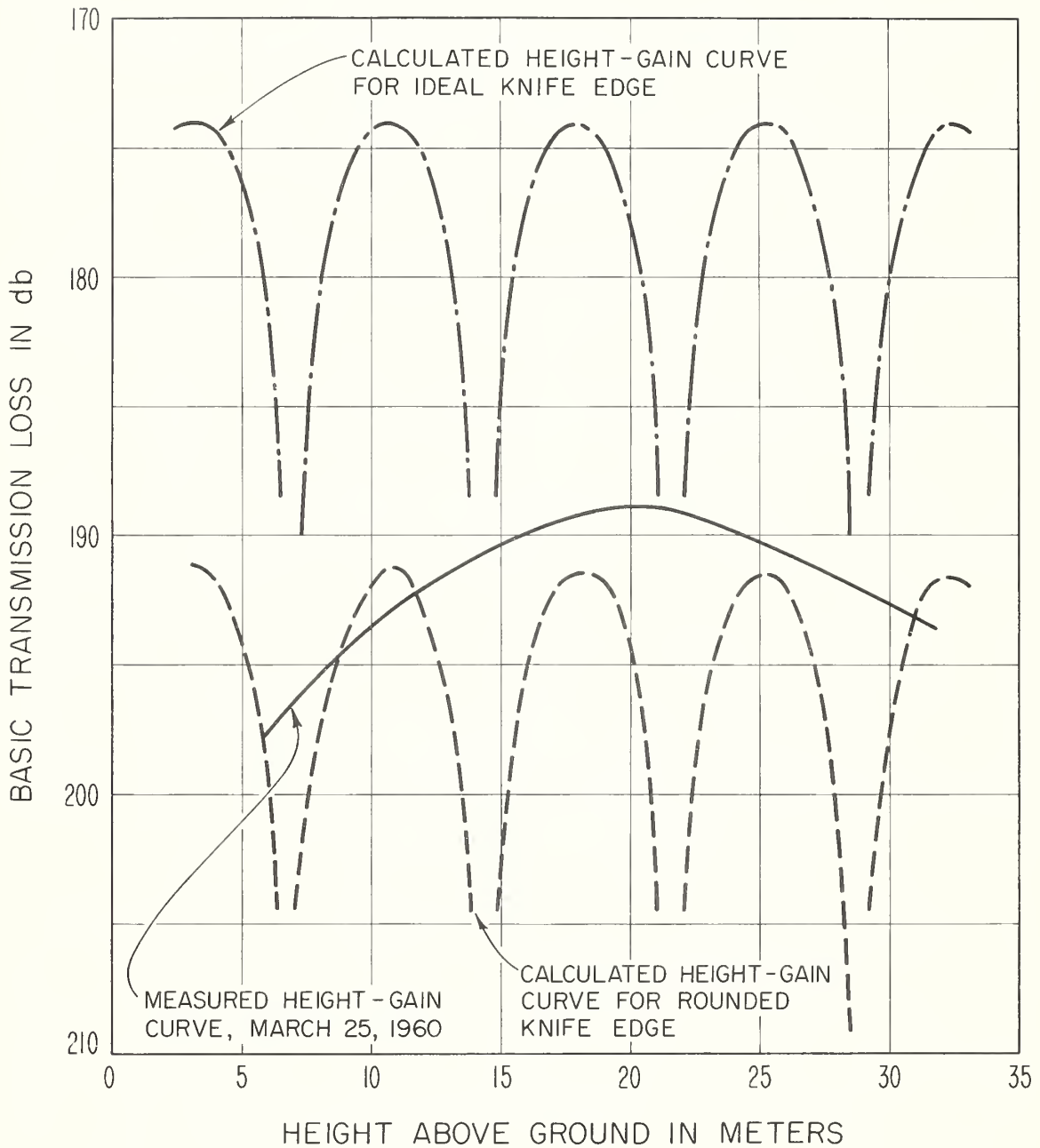


Figure 12

TRANSVERSE PROFILE THROUGH PIKES PEAK
AS SEEN FROM TRANSMITTER SITE

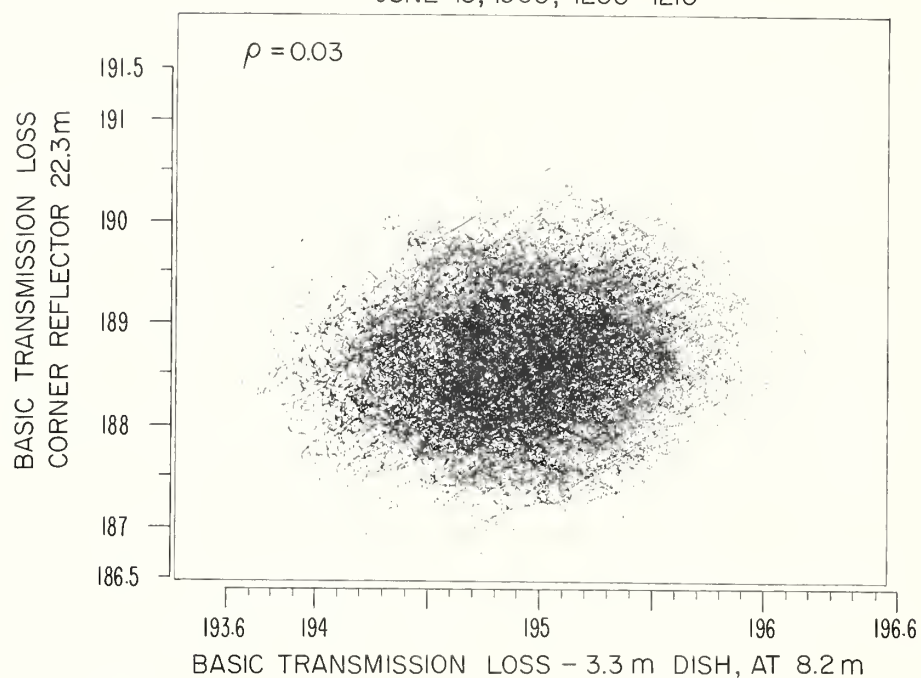


Figure 13

INSTANTANEOUS ENVELOPE CORRELATION
PIKES PEAK OBSTACLE GAIN PATH

751 MC

JUNE 15, 1960; 1200-1210



SEPT. 16, 1960; 1015-1025

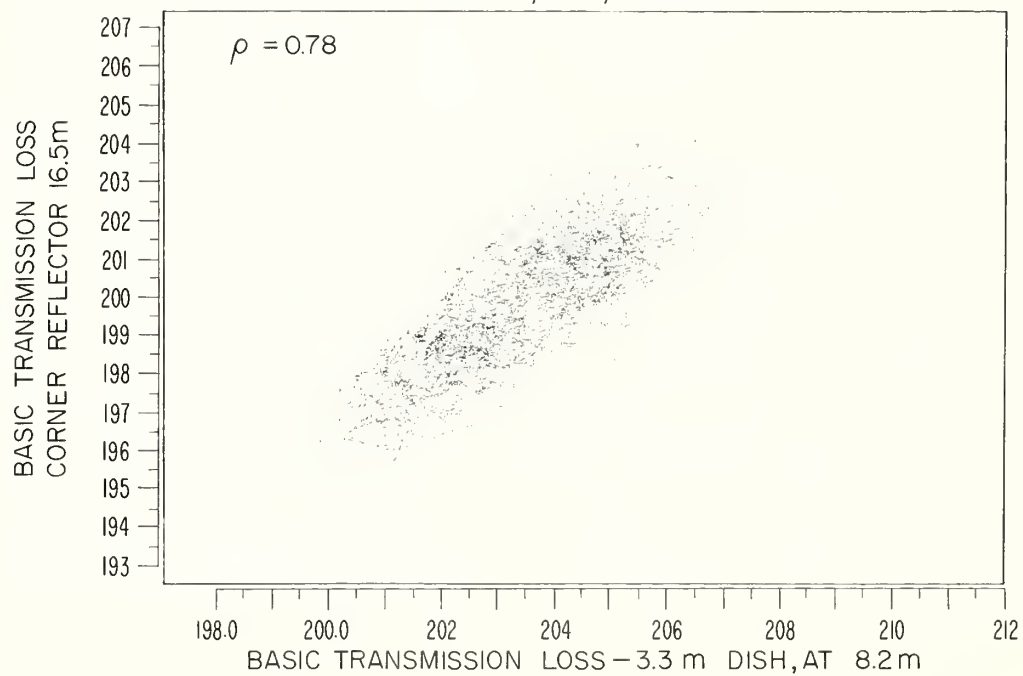


Figure 14

CORRELATION IN HOURLY MEDIANS VERTICALLY SPACED ANTENNAS AT 751 Mc

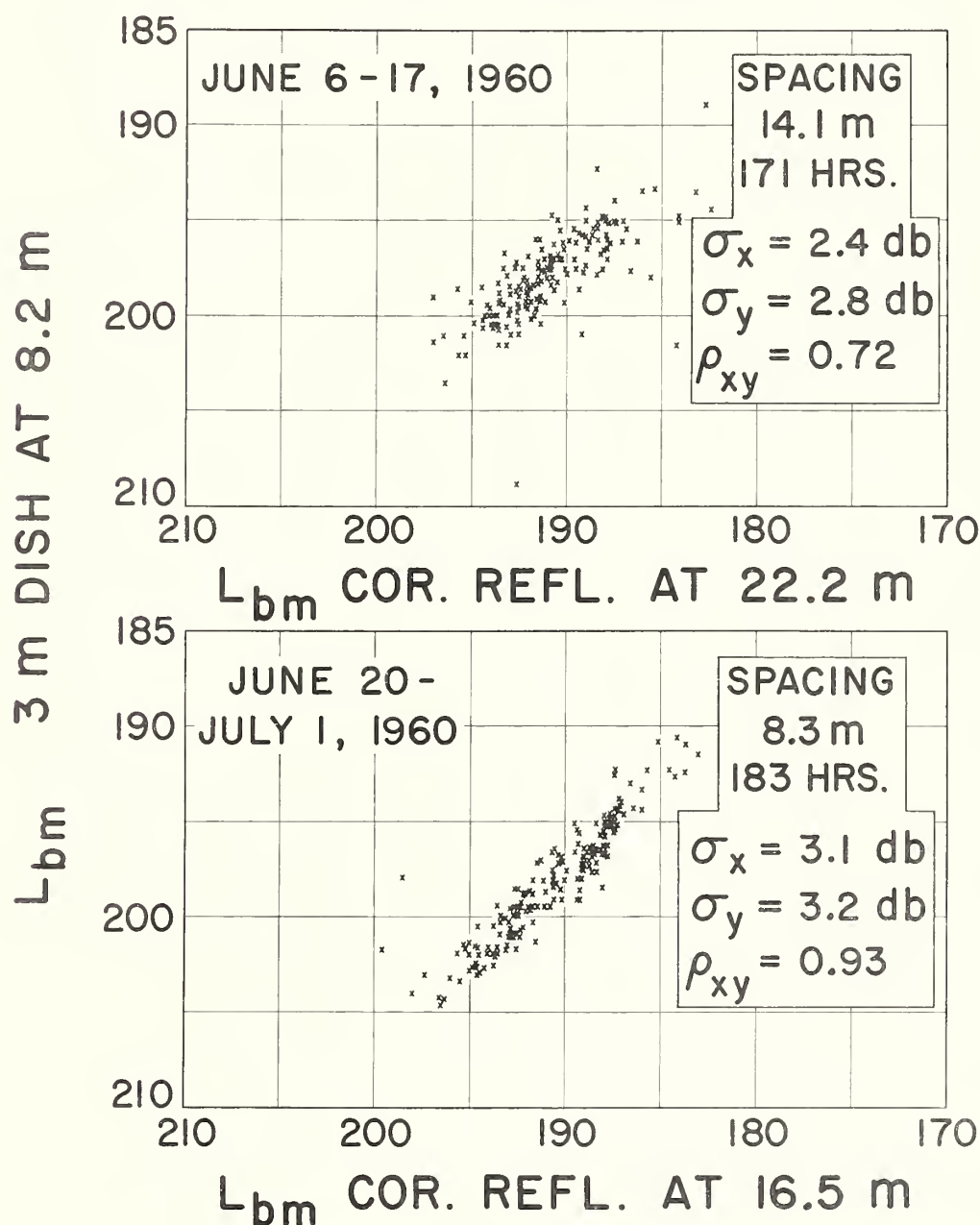


Figure 15

751 MC FADE CHARACTERISTICS OBSERVED ON 3 METER DISH

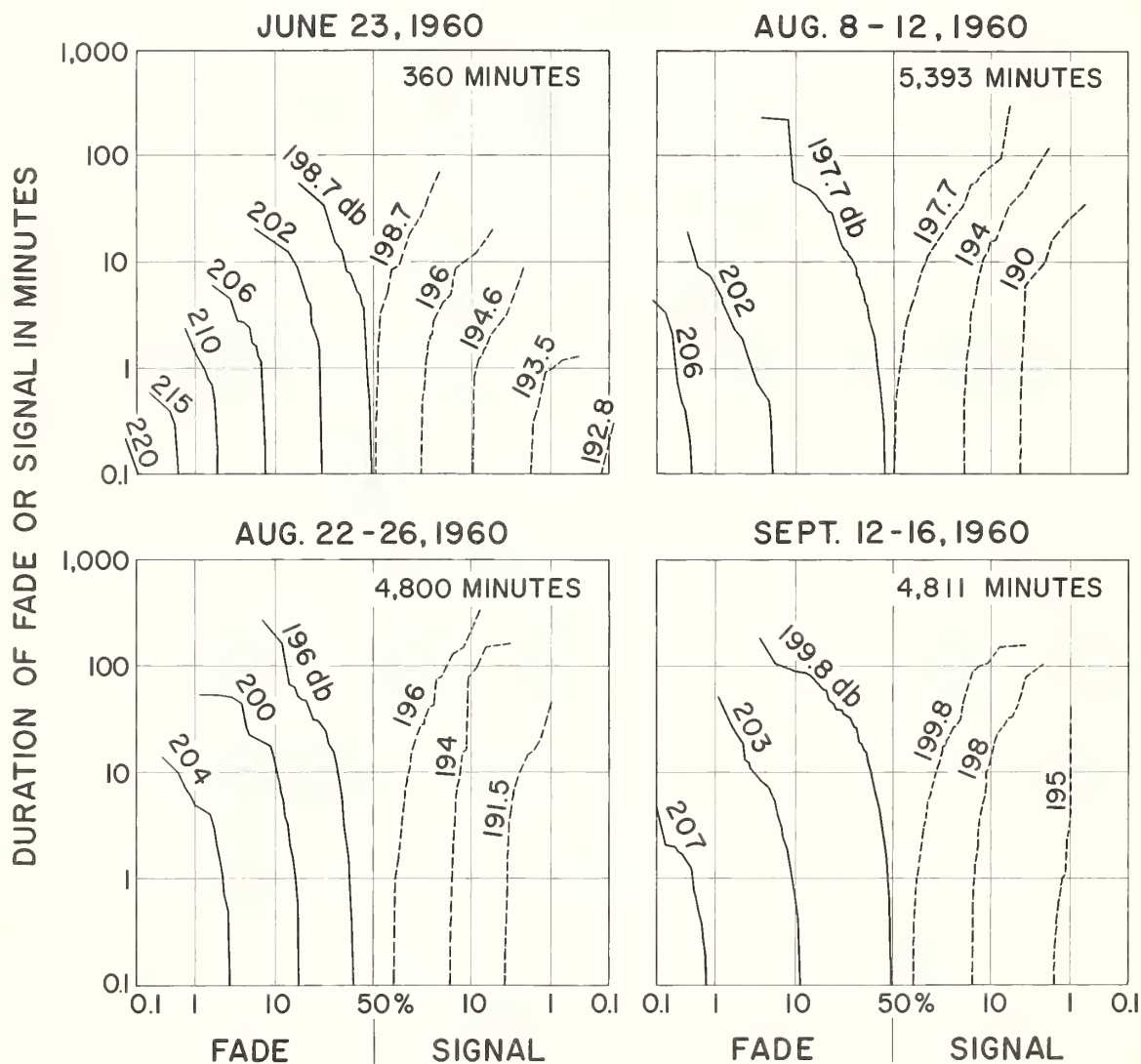


Figure 16

U.S. DEPARTMENT OF COMMERCE

Frederick H. Mueller, *Secretary*

NATIONAL BUREAU OF STANDARDS

A. V. Astin, *Director*



THE NATIONAL BUREAU OF STANDARDS

The scope of activities of the National Bureau of Standards at its major laboratories in Washington, D.C., and Boulder, Colo., is suggested in the following listing of the divisions and sections engaged in technical work. In general, each section carries out specialized research, development, and engineering in the field indicated by its title. A brief description of the activities, and of the resultant publications, appears on the inside of the front cover.

WASHINGTON, D.C.

ELECTRICITY. Resistance and Reactance. Electrochemistry. Electrical Instruments. Magnetic Measurements. Dielectrics.

METROLOGY. Photometry and Colorimetry. Refractometry. Photographic Research. Length. Engineering Metrology. Mass and Scale. Volumetry and Densimetry.

HEAT. Temperature Physics. Heat Measurements. Cryogenic Physics. Rheology. Molecular Kinetics. Free Radicals Research. Equation of State. Statistical Physics. Molecular Spectroscopy.

RADIATION PHYSICS. X-Ray. Radioactivity. Radiation Theory. High Energy Radiation. Radiological Equipment. Nucleonic Instrumentation. Neutron Physics.

CHEMISTRY. Surface Chemistry. Organic Chemistry. Analytical Chemistry. Inorganic Chemistry. Electrodeposition. Molecular Structure and Properties of Gases. Physical Chemistry. Thermochemistry. Spectrochemistry. Pure Substances.

MECHANICS. Sound. Pressure and Vacuum. Fluid Mechanics. Engineering Mechanics. Combustion Controls.

ORGANIC AND FIBROUS MATERIALS. Rubber. Textiles. Paper. Leather. Testing and Specifications. Polymer Structure. Plastics. Dental Research.

METALLURGY. Thermal Metallurgy. Chemical Metallurgy. Mechanical Metallurgy. Corrosion. Metal Physics.

MINERAL PRODUCTS. Engineering Ceramics. Glass. Refractories. Enameled Metals. Constitution and Microstructure.

BUILDING RESEARCH. Structural Engineering. Fire Research. Mechanical Systems. Organic Building Materials. Codes and Safety Standards. Heat Transfer. Inorganic Building Materials.

APPLIED MATHEMATICS. Numerical Analysis. Computation. Statistical Engineering. Mathematical Physics.

DATA PROCESSING SYSTEMS. Components and Techniques. Digital Circuitry. Digital Systems. Analog Systems. Applications Engineering.

ATOMIC PHYSICS. Spectroscopy. Radiometry. Mass Spectrometry. Solid State Physics. Electron Physics. Atomic Physics.

INSTRUMENTATION. Engineering Electronics. Electron Devices. Electronic Instrumentation. Mechanical Instruments. Basic Instrumentation.

Office of Weights and Measures.

BOULDER, COLO.

CRYOGENIC ENGINEERING. Cryogenic Equipment. Cryogenic Processes. Properties of Materials. Gas Liquefaction.

IONOSPHERE RESEARCH AND PROPAGATION. Low Frequency and Very Low Frequency Research. Ionosphere Research. Prediction Services. Sun-Earth Relationships. Field Engineering. Radio Warning Services.

RADIO PROPAGATION ENGINEERING. Data Reduction Instrumentation. Radio Noise. Tropospheric Measurements. Tropospheric Analysis. Propagation-Terrain Effects. Radio-Meteorology. Lower Atmosphere Physics.

RADIO STANDARDS. High frequency Electrical Standards. Radio Broadcast Service. Radio and Microwave Materials. Atomic Frequency and Time Standards. Electronic Calibration Center. Millimeter-Wave Research. Microwave Circuit Standards.

RADIO SYSTEMS. High Frequency and Very High Frequency Research. Modulation Research. Antenna Research. Navigation Systems. Space Telecommunications.

UPPER ATMOSPHERE AND SPACE PHYSICS. Upper Atmosphere and Plasma Physics. Ionosphere and Exosphere Scatter. Airglow and Aurora. Ionospheric Radio Astronomy.

Department of Commerce
National Bureau of Standards
Boulder Laboratories
Boulder, Colorado

Official Business



Postage and Fees Paid
U. S. Department of Commerce